Modern Physics Letters B
Vol. 35, No. 19 (2021) 2150313 (10 pages)

DOI: 10.1142/S0217984921503139

Localized interaction solution and its dynamics of the extended Hirota–Satsuma–Ito equation

Jian-Ping Yu

Department of Applied Mathematics, University of Science and Technology Beijing, Beijing 100083, China

Wen-Xiu Ma[*,†,‡,§,¶] and Chaudry Masood Khalique[¶]

[*] *Department of Mathematics, Zhejiang Normal University, Jinhua 321004, Zhejiang, China*
[†] *Department of Mathematics, King Abdulaziz University, Jeddah, Saudi Arabia*
[‡] *School of Mathematics, South China University of Technology, Guangzhou 510640, China*
[§] *Department of Mathematics and Statistics, University of South Florida, Tampa, FL 33620, USA*
[¶] *International Institute for Symmetry Analysis and Mathematical Modelling, Department of Mathematical Sciences, North-West University, Mafikeng Campus, Private Bag X 2046, Mmabatho 2735, South Africa*

Yong-Li Sun[‖]

Department of Mathematics, Beijing University of Chemical Technology, Beijing 100029, China
sunyl@mail.buct.edu.cn

Received 3 February 2021
Revised 27 February 2021
Accepted 1 March 2021
Published 10 May 2021

In this research, we will introduce and study the localized interaction solutions and their dynamics of the extended Hirota–Satsuma–Ito equation (HSIe), which plays a key role in studying certain complex physical phenomena. By using the Hirota bilinear method, the lump-type solutions will be firstly constructed, which are almost rationally localized in all spatial directions. Then, three kinds of localized interaction solutions will be obtained, respectively. In order to study the dynamic behaviors, numerical simulations are performed. Two interesting physical phenomena are found: one is the fission and fusion phenomena happening during the procedure of their collisions; the other is the rogue wave phenomena triggered by the interaction between a lump-type wave and a soliton wave.

Keywords: Localized interaction solution; dynamic behavior; lump-type solution; the extended Hirota–Satsuma–Ito equation.

[‖]Corresponding author.

1. Introduction

As an important part of soliton theory, which has been applied in many fields such as nonlinear optics, plasmas, solid-state physics and so forth, searching for exact solutions of nonlinear evolution equations (NLEEs) has attracted a lot of attention and has been one of the hot topics,[1–13] such as the construction of rational solutions[14] and other exact solutions.[15–26] In the recent decades, many systematic and effective methods have been proposed for constructing exact solutions, for example, Painlevé analysis method,[27] Darboux transformation method,[28] Bäcklund transformation method,[29] Hirota bilinear method and generalized bilinear approach,[30–33] and inverse scattering method.[34] Among the aforementioned methods, the Hirota direct method is a direct and effective method for constructing exact solutions, which will be used in our research. For example, by using the Hirota direct method, lump and hybrid solutions of NLEEs have been studied by many researchers.[35–42]

Zhou *et al.*,[43] applied the Hirota direct method to construct lump and interaction solutions to the $(2+1)$-dimensional Hirota–Satsuma–Ito (HSI) equation. Moreover, Ma[44] and Liu *et al.*[45] constructed the lump and lump-soliton interaction solutions of an $(2+1)$-dimensional extension of the HSI equation. These research works motivate us to generalize the (2+1)-dimensional cases to the following (3+1)-dimensional case, which can be applied to study shallow water:

$$w_t = u_{xxt} + 3uu_t - 3u_x v_t + \alpha u_x, \quad w_x = -u_y - u_z, \quad v_x = -u. \tag{1}$$

To the best of our knowledge, for the first time, Eq. (1) is introduced and there is no reference about Eq. (1) elsewhere.

The task of this research is to obtain the interaction solution and its dynamics of Eq. (1) based on the Hirota bilinear method. In the meanwhile, numerical simulations are performed graphically, which show that choosing parameters has big impact on the types and dynamic properties of the solutions. Since the structure of the $(3+1)$-dimensional equation (1) is more complex and complicated than the $(2+1)$-dimensional models, then the obtained results in this paper are significantly richer than those derived about the $(2+1)$-dimensional equations[44] and Ref. 45.

This paper is organized as follows. In Sec. 2, localized lump-type solutions are given to the $(3+1)$-dimensional equation (1), wherein the dynamic behaviors are graphically analyzed in detail. In Secs. 3–5, three kinds of interaction solutions are constructed: the first consisting of a lump-type and a stripe soliton waves, the second is the combination of a lump-type and a periodic waves, the last is the interaction between a lump-type and a pair of kink waves. Due to the complex structure of $(3+1)$-dimensional models and the tedious computations, we only provide three kinds of interaction solutions. And the numerical simulations are given through the corresponding graphs. Finally, some discussions are given in Sec. 6.

2. Lump-Type Solution

In order to construct the lump-type solutions of Eq. (1), by using the logarithmic transformation $u = 2(\ln f(x, y, z, t))_{xx}$, we firstly turn Eq. (1) into the following Hirota bilinear form:

$$(D_t D_x^3 + D_t D_y + D_t D_z + \alpha D_x^2)(f \cdot f) = 0, \tag{2}$$

where $\alpha \neq 0$ is a real constant and D_x, D_t, D_y, D_z are the Hirota derivatives defined by

$$\begin{aligned} &D_x^m D_y^n D_z^l a(x, y, z) \cdot b(x, y, z) \\ &\quad = \left(\frac{\partial^m}{\partial s^m} \frac{\partial^n}{\partial t^n} \frac{\partial^l}{\partial r^l} \right) a(x + s, y + t, z + r) b(x - s, y - t, z - r)|_{s=0,t=0,r=0}, \\ &\qquad m, n, l = 0, 1, 2, 3, \ldots. \end{aligned} \tag{3}$$

According to the quadratic function method,[36] function f in Eq. (2) is as follows:

$$f = g^2 + h^2 + a_{11} \tag{4}$$

with

$$g = a_1 x + a_2 y + a_3 z + a_4 t + a_5, \quad h = a_6 x + a_7 y + a_8 z + a_9 t + a_{10}, \tag{5}$$

where a_i's are real parameters to be determined later. Now, plugging (4) into (2) and setting the coefficients of x, y, z, t to zero yield a solution of parameters a_i's as follows:

$$\begin{aligned} a_2 &= -\frac{(\alpha a_1^2 a_4 + 2\alpha a_1 a_6 a_9 - \alpha a_4 a_6^2 + a_3 a_4^2 + a_3 a_9^2)}{(a_4^2 + a_9^2)}, \\ a_7 &= \frac{\alpha a_1^2 a_9 - 2\alpha a_1 a_4 a_6 - \alpha a_6^2 a_9 - a_4^2 a_8 - a_8 a_9^2}{a_4^2 + a_9^2}, \\ a_{11} &= \frac{\begin{array}{l} -3(a_1^3 a_4^3 + a_1^3 a_4 a_9^2 + a_1^2 a_4^2 a_6 a_9 + a_1^2 a_6 a_9^3 + a_1 a_4^3 a_6^2 \\ \quad + a_1 a_4 a_6^2 a_9^2 + a_4^2 a_6^3 a_9 + a_6^3 a_9^3) \end{array}}{\alpha(a_1 a_9 - a_4 a_6)^2}, \end{aligned} \tag{6}$$

which satisfy the following constraint conditions:

$$a_1 a_9 - a_4 a_6 \neq 0, \quad a_4^2 + a_9^2 \neq 0, \tag{7}$$

which make sure that $u = 2(\ln f(x, y, z, t))_{xx}$ is well defined. The above-mentioned solution of a_i's in (6) leads to a positive quadratic function solution of (2), which, in turn, yields a lump-type solution of (1) given by

$$u = 2(\ln f)_{xx} = \frac{4((a_1^2 + a_4^2) f - 2(a_1 g + a_4 h)^2)}{f^2} \tag{8}$$

with functions g and h defined in (5). As a matter of fact, the solution (8) is a lump solution if and only if $u \to 0$ while $x^2 + y^2 + z^2 \to \infty$. But the solution (8) does

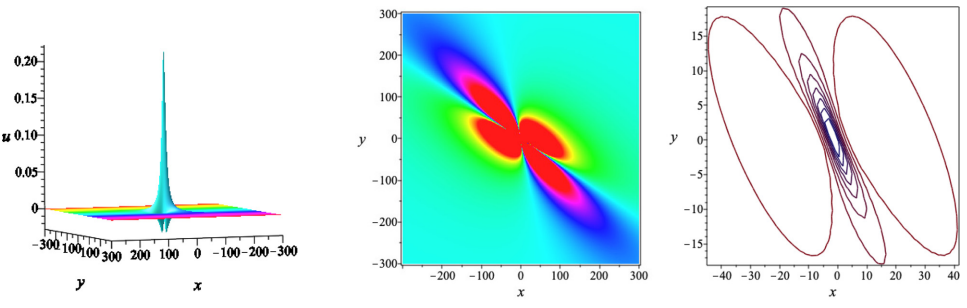

(a) (b) (c)

Fig. 1. (Color online) Profile of the bright lump-type solution u in (8) with $t = 0, z = 1$ at different time. The specific parameters are $\alpha = -1, a_1 = 2, a_3 = 1, a_4 = 1, a_5 = 1, a_6 = 1, a_8 = 1, a_9 = 1, a_{10} = 1$. (a) 3D plot; (b) Density plot; (c) Contour plot.

not go to zero along any direction in the space of x, y, z because of the special and complicated characters of $(3+1)$-dimensions in the resulting solution. For example, when $x^2 + y^2 + z^2 \to \infty$ in the direction of the intersection line of surfaces $g = 0$ and $h = 0$, the solution (8) goes to a nonzero constant $\frac{4(a_1^2+a_4^2)}{a_{11}} \neq 0$ for $a_1^2 + a_4^2 \neq 0$ and $a_{11} \neq 0$. Hence, it is only a lump-type solution not a lump solution.

The corresponding numerical simulations are given graphically by choosing specific parameters $\alpha = -1, t = 0, z = 1, a_1 = 2, a_3 = 1, a_4 = 1, a_5 = 1, a_6 = 1, a_8 = 1, a_9 = 1, a_{10} = 1$. By the tedious computations in Maple, we see that the solution u in (8) has one maximum point $(-\frac{2}{7}, \frac{4}{7}, 1)$ and two minimum points $(-\frac{12}{7} \pm \frac{\sqrt{6}}{3}, \frac{4}{7}, 1)$. Therefore, there is one peak corresponding to the maximum point and two valleys corresponding to the two minimum points. Moreover, this solution u in (8) is a bright lump-type solution since the height of the peak is bigger than the depth of the two valley bottoms.

3. Localized Interaction Solutions

In recent years, based on the extensive investigation of exact solutions of NLEEs, the study of interaction solutions among nonlinear excitations of integrable or non-integrable systems has been paid a lot of attention since interaction solutions have more interesting features and important applications. To construct the hybrid solution between a lump-type and a soliton solution, function f is taken in the form

$$f = g^2 + h^2 + ke^{\beta} + a_{15} \tag{9}$$

with

$$\begin{aligned} g &= a_1x + a_2y + a_3z + a_4t + a_5, \\ h &= a_6x + a_7y + a_8z + a_9t + a_{10}, \\ \beta &= a_{11}x + a_{12}y + a_{13}z + a_{14}t, \end{aligned} \tag{10}$$

where a_i's and k are real parameters to be determined. By substituting (9) into (2), the solutions of these parameters are obtained as

$$a_1 = \frac{3a_9a_{11}^2}{2\alpha}, \quad a_2 = -\frac{3a_6a_{11}^2}{2}, \quad a_3 = 0, \quad a_4 = -\frac{2\alpha a_6}{3a_{11}^2}, \quad a_7 = \frac{9a_9a_{11}^4}{4\alpha},$$
$$a_8 = 0, \quad a_{10} = -\frac{3a_5a_9a_{11}^2}{2\alpha a_6}, \quad a_{12} = \frac{1}{2}a_{11}^3 - a_{13}, \quad a_{14} = -\frac{2\alpha}{3a_{11}}, \quad a_{15} = 0 \tag{11}$$

satisfying the condition $a_6a_{11} \neq 0$, which is a sufficient and necessary condition for the solution u to be well defined. Without loss of generality, selecting appropriate parameters, $\alpha = 1, k = 1, a_5 = 1, a_6 = -1, a_7 = -1, a_9 = -1, a_{11} = -1, a_{13} = -1, a_{14} = 1$, yields the corresponding solution u with $t = 0$ and $z = 1$

$$\begin{aligned} u &= 2(\ln(g + h + ke^{\beta} + a_{15}))_{xx} \\ &= \frac{2(g_{xx} + h_{xx} + (ke^{\beta}_{xx})) - 2(g_x + h_x + (ke^{\beta})_x)^2}{(g + h + ke^{\beta})^2}. \end{aligned} \tag{12}$$

Then the interaction phenomena between a lump-type wave and a strip soliton wave are as shown by Fig. 2. It is noted that the lump-type wave is firstly hidden in the stripe soliton wave (see Fig. 2(a)). From Fig. 2(a), since it travels faster than the stripe soliton wave with slow velocity, we can see that the stripe soliton begins to split up into one lump-type wave, which implies that the fission phenomenon happens. In Fig. 2(c), it is noted that it has totally run away from the stripe soliton wave and keeps propagating along the negative direction of the y-axis. The mathematical reason is that the solution u consists of two parts: a polynomial function and an exponential function, which plays a more important role than the polynomial part. Moreover, we found that the polynomial part of u has nothing to do with spatial variable z.

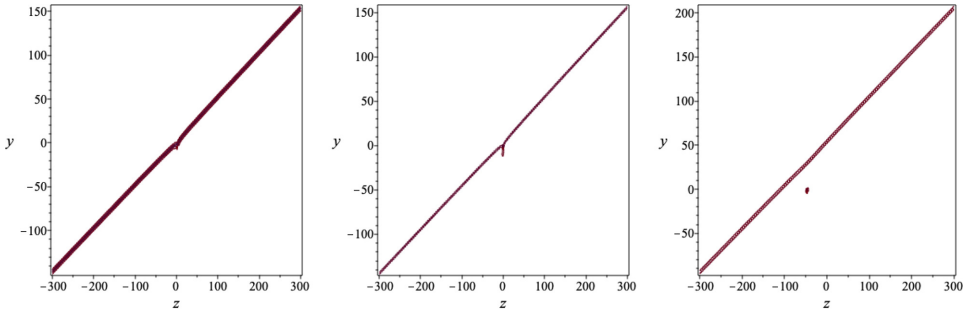

(a) (b) (c)

Fig. 2. (Color online) Profile of the bright lump-type solution u in (8) with $z = 1$ at different time. The specific parameters are $\alpha = -1, a_1 = 2, a_3 = 1, a_4 = 1, a_5 = 1, a_6 = 1, a_8 = 1, a_9 = 1, a_{10} = 1$. (a) $t = -5$; (b) $t = 0$; (c) $t = 100$.

4. Interaction Between a Lump-Type Solution and a Periodic Solution

In this section, to obtain the interaction solution between a lump-type and a periodic solution, the form of function f in (2) as a combination of a periodic function and a positive quadratic polynomial function is

$$f = g^2 + h^2 + k\cos\beta + a_{15} \tag{13}$$

with

$$\begin{aligned} g &= a_1x + a_2y + a_3z + a_4t + a_5, \\ h &= a_6x + a_7y + a_8z + a_9t + a_{10}, \\ \beta &= a_{11}x + a_{12}y + a13z + a_{14}t, \end{aligned} \tag{14}$$

where a_i's and k are all real parameters to be determined. Substituting (3) into the bilinear form (2) leads to the constraint conditions among the parameters as

$$\begin{gathered} a_1 = -\frac{3a_9a_{11}^2}{2\alpha}, \quad a_2 = \frac{3a_6a_{11}^2}{2}, \quad a_3 = 0, \quad a_4 = \frac{2\alpha a_6}{3a_{11}^2}, \\ a_7 = \frac{9a_9a_{11}^4}{4\alpha}, \quad a_8 = 0, \quad a_{10} = \frac{3a_5a_9a_{11}^2}{2\alpha a_6}, \quad a_{12} = -\frac{a_{11}^3}{2} - a_{13}, \\ a_{14} = \frac{2\alpha}{3a_{11}}, \quad a_{15} = -\frac{2\alpha^2k^2a_{11}^2}{9a_9^2a_{11}^4 + 4\alpha^2a_6^2} \end{gathered} \tag{15}$$

satisfying $a_{11}a_6 \neq 0$, which is a guarantee that the solution u of (1) is well defined. If we take the above-mentioned parameters as $\alpha = 1, k = 1, a_5 = 1, a_6 = -1, a_7 = -1, a_9 = -1, a_{11} = -1, a_{13} = -1, a_{14} = 1$, the solution at $t = 0$ and $y = 1$ is given as follows:

$$\begin{aligned} u &= 2(\ln(g + h + ke^{\beta} + a_{15}))_{xx} \\ &= \frac{2(g_{xx} + h_{xx} + (k\cos(\beta))_{xx}) - 2(g_x + h_x + (k\cos(\beta))_x)^2}{(g + h + k\cosh(\beta))^2}. \end{aligned} \tag{16}$$

From (15) and (16), the polynomial part of the solution u in (16) has nothing to do with the spatial variable z but the coefficient of the spatial variable z in the periodic part is not equal to zero. The interaction phenomena between a lump-type and a strip soliton wave are illustrated in Fig. 3. From Fig. 3, at time of $t = 0$, we see that the solution u in (16) has different shapes on different coordinate planes, for example, the shape of u on the xOy plane is a lump wave, but the shapes of u on other two coordinate planes look like the complex dark period solitons.

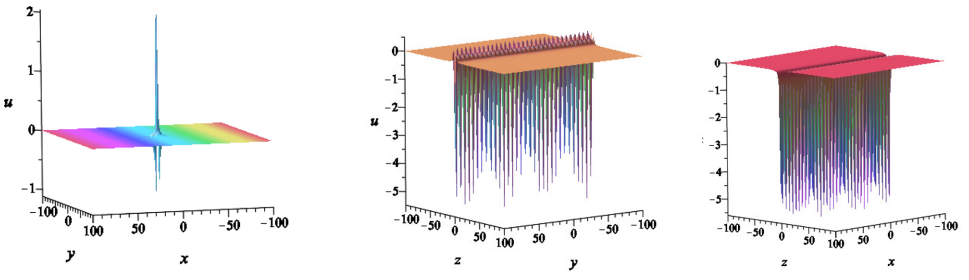

(a) (b) (c)

Fig. 3. (Color online) Evolution profile of the interaction solution u in (16) with $t = 0$. The specific parameters are $\alpha = 1, k = 1, a_5 = 1, a_6 = -1, a_7 = -1, a_9 = -1, a_{11} = -1, a_{13} = -1, a_{14} = 1$. (a) 3D plot on xOy plane; (b) 3D plot on yOz plane; (c) 3D plot on xOz plane.

5. Interaction Between a Lump-Type Solution and a Pair of Kink Solutions

In order to study the interaction solution between a lump-type solution and a pair of kink solutions, function f in (2) is taken to be a combination of a hyperbolic cosine function and a positive quadratic polynomial function as

$$f = g^2 + h^2 + k\cosh\beta + a_{15} \tag{17}$$

with

$$\begin{aligned} g &= a_1x + a_2y + a_3z + a_4t + a_5, \\ h &= a_6x + a_7y + a_8z + a_9t + a_{10}, \\ \beta &= a_{11}x + a_{12}y + a_{13}z + a_{14}t, \end{aligned} \tag{18}$$

where parameters a_i's and k are real to be determined. By putting (17) into the bilinear equation (2), the corresponding relations are

$$\begin{aligned} k &= \frac{9a_9^2a_{11}^4 + 16\alpha^2a_1^2}{8a_{11}^2\alpha^2}, \quad a_2 = -\frac{3a_{11}^2(9a_9^2a_{11}^4 + 16\alpha^2a_1^2 + 16\alpha a_7a_9}{64a_1\alpha^2}, \\ a_3 &= \frac{3(9a_9a_{11}^4 + 16\alpha a_7))a_9a_{11}^2}{64a_1\alpha^2}, \quad a_4 = \frac{4\alpha a_1}{3a_{11}^2}, \quad a_6 = \frac{3a_9a_{11}^2}{4\alpha}, \\ a_8 &= -\frac{9a_9a_{11}^4 + 16\alpha a_7}{16\alpha}, \quad a_{12} = -\frac{1}{4}a_{11}^3 - a_{13}, \quad a_{14} = -\frac{4\alpha}{3a_{11}} \end{aligned} \tag{19}$$

satisfying $a_{11} \neq 0$, which guarantees the solution u of (1) be well defined. Now, choosing the parameters $\alpha = 1, a_1 = 1, a_5 = 1, a_7 = 1, a_9 = 1, a_{10} = 1, a_{11} = 1, a_{13} = 1, a_{15} = 1$, we have the solution u at time $t = 0$ and $z = 1$ as follows:

$$\begin{aligned} u &= 2(\ln(g + h + k\cosh(\beta) + a_{15}))_{xx} \\ &= \frac{2(g_{xx} + h_{xx} + (k\cosh(\beta))_{xx}) - 2(g_x + h_x + (k\cosh(\beta))_x)^2}{(g + h + k\cosh(\beta))^2}. \end{aligned} \tag{20}$$

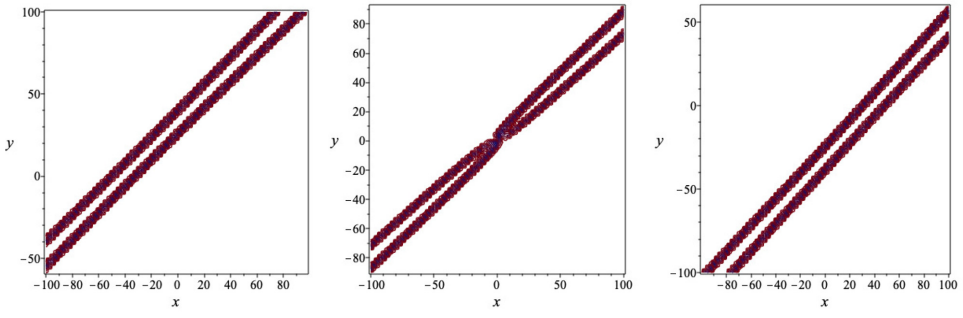

(a) (b) (c)

Fig. 4. (Color online) Evolution profile of the interaction solution u in (1) with $t = 0, z = 1$. The specific parameters are $\alpha = 1, a_1 = 1, a_5 = 1, a_7 = 1, a_9 = 1, a_{10} = 1, a_{11} = 1, a_{13} = 1, a_{15} = 1$. (a) Contour plot at $t = -30$; (b) Contour plot at $t = 0$; (c) Contour plot at $t = 30$.

The numerical simulation of Eq. (20) is given by Fig. 4. During the interaction progress, only a pair of kink waves exists, as shown in Fig. 4(a), as a matter of fact, the lump-type solution is hiding itself in one of this pair of kink waves. In Fig. 4(b), the collisions happened among the lump-type solution and the kink waves since the kink wave in which the lump-type wave is hiding itself travels faster than the other kink wave. Figure 4(c) shows that the kink waves which carry the lump-type wave and the other kink wave are separated from each other and keep traveling forward.

6. Discussions

The extended HSIe (1) is a physical model of very importance, since it has richer dynamic properties due to its complex structure. In this paper, by using the Hirota direct method, lump-type solutions are constructed. And then three kinds of localized interaction solutions are also obtained. Moreover, numerical analysis is implemented on the dynamic behaviors and the propagation properties are obtained. All the numerical simulations show that the dynamic behaviors of the solutions are much richer and the types of parameters chosen have a very big impact on the propagation properties, which can be seen from Figs. 2–4. Due to the complexity of selecting the parameters and the complex structure of the $(3 + 1)$-dimensional model, it is very hard to study the interaction solutions, however, they are worthy of being investigated since they play a key role in physics. Therefore, in the future, we will study other interaction solutions, such as the hybrid solutions between a high-order breather and a line-soliton, and how the related parameters affect the complex dynamic behaviors of the interaction solutions. The method used in this paper can be used to construct solutions of other nonlinear physical models. Moreover, the results obtained in this paper may provide a potential technique to study other localized waves.

Acknowledgment

This work is supported by the National Natural Science Foundation of China (Nos. 11971067 and 11101029).

References

1. D. S. Wang and J. Liu, *Appl. Math. Lett.* **79** (2018) 211.
2. X. Z. Hao, Y. P. Liu, X. Y. Tang, Z. B. Li and W. X. Ma, *Mod. Phys. Lett. B* **32**(27) (2018) 1850332.
3. X. L. Yong, Y. J. Fan, Y. H. Huang, W. X. Ma and J. Tian, *Mod. Phys. Lett. B* **31**(30) (2017) 1750276.
4. B. Ren, X. P. Cheng and J. Lin, *Nonlinear Dyn.* **86** (2016) 1855.
5. J. P. Yu, F. D. Wang, W. X. Ma, Y. L. Sun and C. M. Khalique, *Nonlinear Dyn.* **25** (2019) 1687.
6. H. Wang, Y. H. Wang, W. X. Ma and C. Temuer, *Mod. Phys. Lett. B* **32**(31) (2018) 1850376.
7. J. P. Yu, W. X. Ma, B. Ren, Y. L. Sun and C. M. Khalique, *Complexity* **2019** (2019) 5874904.
8. J. P. Yu and Y. L. Sun, *Nonlinear Dyn.* **87** (2017) 2755.
9. D. S. Wang and X. L. Wang, *Nonlinear Anal. Real World Appl.* **41** (2018) 334.
10. J. P. Yu, W. X. Ma, Y. L. Sun and C. M. Khalique, *Mod. Phys. Lett. B* **32**(33) (2018) 1850409.
11. B. Ren, *Phys. Scr.* **90** (2015) 065206, http://iopscience.iop.org/article/10.1088/0031-8949/90/6/065206.
12. D. S. Wang, B. L. Guo and X. L. Wang, *J. Differ. Eqn.* **266** (2019) 5209.
13. Y. L. Sun, W. X. Ma, J. P. Yu and C. M. , *Mod. Phys. Lett. B* **32**(24) (2018) 1850282.
14. B. Ren, W. X. Ma and J. Yu, *Nonlinear Dyn.* **96** (2019) 717.
15. S. J. Chen, Y. H. Yin, W. X. Ma and X. Lü, *Anal. Math. Phys.* **9** (2019) 2329.
16. J. W. Xia, Y. W. Zhao and X. Lü, *Commun. Nonlinear Sci. Numer. Simul.* **88** (2020) 105260.
17. Y. H. Yin, S. J. Chen and X. Lü, *Chin. Phys. B* **29** (2020) 120502.
18. X. Lü, Y. F. Hua, S. J. Chen and X. F. Tang, *Commun. Nonlinear Sci. Numer. Simul.* **95** (2021) 105612.
19. S. J. Chen, X. Lü and X. F. Tang, *Commun. Nonlinear Sci. Numer. Simul.* **95** (2021) 105628.
20. X. Lü and S. J. Chen, *Nonlinear Dyn.* **103** (2021) 947.
21. H. N. Xu, W. Y. Ruan, Y. Zhang and X. Lü, *Appl. Math. Lett.* **99** (2020) 105976.
22. X. Lü, S.-T. Chen and W.-X. Ma, *Nonlinear Dyn.* **86** (2016) 523.
23. L. Xu, D. S. Wang, X. Y. Wen and Y. L. Jiang, *J. Nonlinear Sci.* **30** (2020) 537.
24. Y. H. Yin, W. X. Ma, J. G. Liu and X. Lü, *Comput. Math. Appl.* **76** (2018) 1275.
25. M. Li, M. Li and J. S. He, *Nonlinear Dyn.* **102** (2020) 1825.
26. S. J. Chen, W. X. Ma and X. Lü, *Commun. Nonlinear Sci. Numer. Simul.* **83** (2020) 105135.
27. J. Weiss, M. Tabor and G. Carnevale, *J. Math. Phys.* **24** (1983) 522.
28. V. B. Matveev and M. A. Salle, *Darboux Transformations and Solitons* (Springer-Verlag, Berlin, 1991).
29. D. J. Kaup, *J. Math. Phys.* **22** (1981) 1176.
30. R. Hirota, *The Direct Method in Soliton Theory* (Cambridge University Press, New York, 2004).
31. B. Ren, J. Lin and Z. W. Lou, *Appl. Math. Lett.* **105** (2020) 106326.

32. R. Hirota, *Phys. Rev. Lett.* **27** (1971) 1192.
33. W. X. Ma, *Stud. Nonlinear Sci.* **2** (2011) 140.
34. M. J. Ablowitz and P. A. Clarkson, *Solitons, Nonlinear Evolution Equations and Inverse Scattering* (Cambridge University Press, New York, 1991).
35. R. S. Johnson and S. Thompson, *Phys. Lett. A* **66** (1978) 278.
36. W. X. Ma, *Phys. Lett. A* **379** (2015) 1975.
37. W. X. Ma and Y. Zhou, *J. Differ. Equations* **264** (2018) 2633.
38. J. G. Liu and Y. He, *Nonlinear Dyn.* **92** (2018) 1103.
39. W. X. Ma, X. L. Yong and H. Q. Zhang, *Comput. Math. Appl.* **75** (2018) 289.
40. J. P. Yu and Y. L. Sun, *Nonlinear Dyn.* **87** (2017) 1405.
41. J. P. Yu, J. Jing, Y. L. Sun and S. P. Wu, *Appl. Math. Comput.* **273** (2016) 697.
42. W. X. Ma, *J. Appl. Anal. Comput.* **9** (2019) 1319.
43. Y. Zhou, S. Manukure and W. X. Ma, *Commun. Nonlinear Sci. Numer. Simul.* **68** (2019) 56, doi:10.1016/j.cnsns.2018.07.038.
44. W. X. Ma, *Front. Math. China* **14** (2019) 619.
45. Y. Q. Liu, X. Y. Wen and D. S. Wang, *Comput. Math. Appl.* **77** (2019) 947.